TABLE III. Summary of results.

Isotope	$B(E2, 0^+\rightarrow 2^+)$ in e^2 b^2 Present expt	Casten *et al.*[a]	K-B[b]	Q_2^+ in e b Present expt (P_4 positive)	Present expt (P_4 negative)	Mössbauer expt[c]	K-B[b] (P_4 negative)	Rot. model
Os^{188}	2.90±0.08	2.70±0.40	2.731	−0.39±0.38	−1.31±0.34	−1.81±0.24	−1.160	(−)1.52
Os^{190}	2.39±0.06	2.50±0.27	2.595	+0.27±0.12	−0.99±0.13		−0.891	(−)1.40
Os^{192}	2.04±0.06	2.22±0.34	2.576	1.22±0.19	−0.41±0.20		−0.359	(−)1.29

[a] Results of Ref. 2.
[b] Prediction of Kumar-Baranger theory, Ref. 1.
[c] See Ref. 9.

Mössbauer result for Os^{188} which is independent of the sign of P_4 is consistent with our value corresponding to P_4 negative. This strongly suggests that P_4 is indeed negative as predicted by Kumar.[7] Figure 3 demonstrates that this solution is also in rather good agreement with the Kumar-Baranger theory. The rotational values for Q_2^+ listed in the last column of Table III are for Os^{190} and Os^{192} inconsistent with experiment.

ACKNOWLEDGMENTS

We want to thank both J. R. Kerns and S. L. Lane for stimulating discussions and extensive help in data taking. We greatly benefited from discussions and correspondence with Professor K. Kumar, Professor M. Baranger, and Professor K. Alder. It is a pleasure to acknowledge the expert help and cooperation of our accelerator crew.

PHYSICAL REVIEW C VOLUME 1, NUMBER 4 APRIL 1970

$Pb^{208}(d, \alpha)Tl^{206}$ Reaction and the $\pi^{-1}\nu^{-1}$ Structure of Tl^{206}†

M. B. LEWIS* AND W. W. DAEHNICK
Nuclear Physics Laboratory, University of Pittsburgh, Pittsburgh, Pennsylvania 15213

(Received 20 October 1969)

The proton-neutron hole states of Tl^{206} have been studied by the direct $Pb^{208}(d, \alpha)Tl^{206}$ reaction with 17-MeV deuterons. Experimental resolutions of 12–15 keV for about 28-MeV α particles permitted the investigation of many two-hole states previously unknown. For most levels, L values could be extracted from the comparison of microscopic two-nucleon transfer distorted-wave Born-approximation (DWBA) calculations with experimental angular distributions. The experimental level energies and J^π assignments (or limits) were compared where possible to recent (n, γ) and (t, α) data for Tl^{206}, and to structure calculations by Kuo. It was possible to correlate about 20 low-lying levels ($E_x \lesssim 2.2$ MeV) with calculated shell-model states. In addition, Kuo's wave functions were used to derive detailed (d, α) cross-section intensity distributions, and to check the dependence of the absolute normalization constant $N(d, \alpha)$ on various DWBA parameters. Constructive coherence in the transition amplitudes predicted by the wave functions for the lowest states of a given J^π was varified experimentally. Ten enhanced (d, α) cross sections are observed, in good qualitative agreement with theoretical predictions. The predicted enhancement for the population of some of these states was occasionally in excess of the observed enhancement.

I. INTRODUCTION

ONE of the simplest ways in which the two-nucleon force manifests itself in nuclear structure is through the residual interaction in nuclei with two holes in a stable closed-shell core. It was the purpose of the present study to experimentally examine and interpret the proton-neutron hole states of Tl^{206}. The doubly magic Pb^{208} ground state is well known to be the best vacuum (i.e., inert) state of any nucleus and serves as an ideal nuclear core for single-particle orbitals.[1] The residual interaction between the proton hole and the neutron hole depends on both the $T=0$ and $T=1$ components of the nucleon-nucleon scattering potential, and determines the configuration admixtures into the $\pi^{-1}\nu^{-1}$ wave functions of Tl^{206}, and the splitting of the $\pi^{-1}\nu^{-1}$ multiplets.

In this work, we probe these two-hole states primarily by studying the $Pb^{208}(d, \alpha)Tl^{206}$ reaction, which is expected to excite almost all the low-lying $\pi^{-1}\nu^{-1}$ states. The strength of this deuteron pickup transition to the various $\pi^{-1}\nu^{-1}$ states depends upon all final-state con-

† Work supported by the National Science Foundation.
* Present address: Nuclear Data Group, Oak Ridge National Laboratory, Oak Ridge, Tenn.

[1] W. C. Parkinson, D. L. Hendrie, H. H. Duhm, J. Mahoney, J. Saundinos, and G. G. R. Satchler, Phys. Rev. **178**, 1976 (1969). See also references therein.

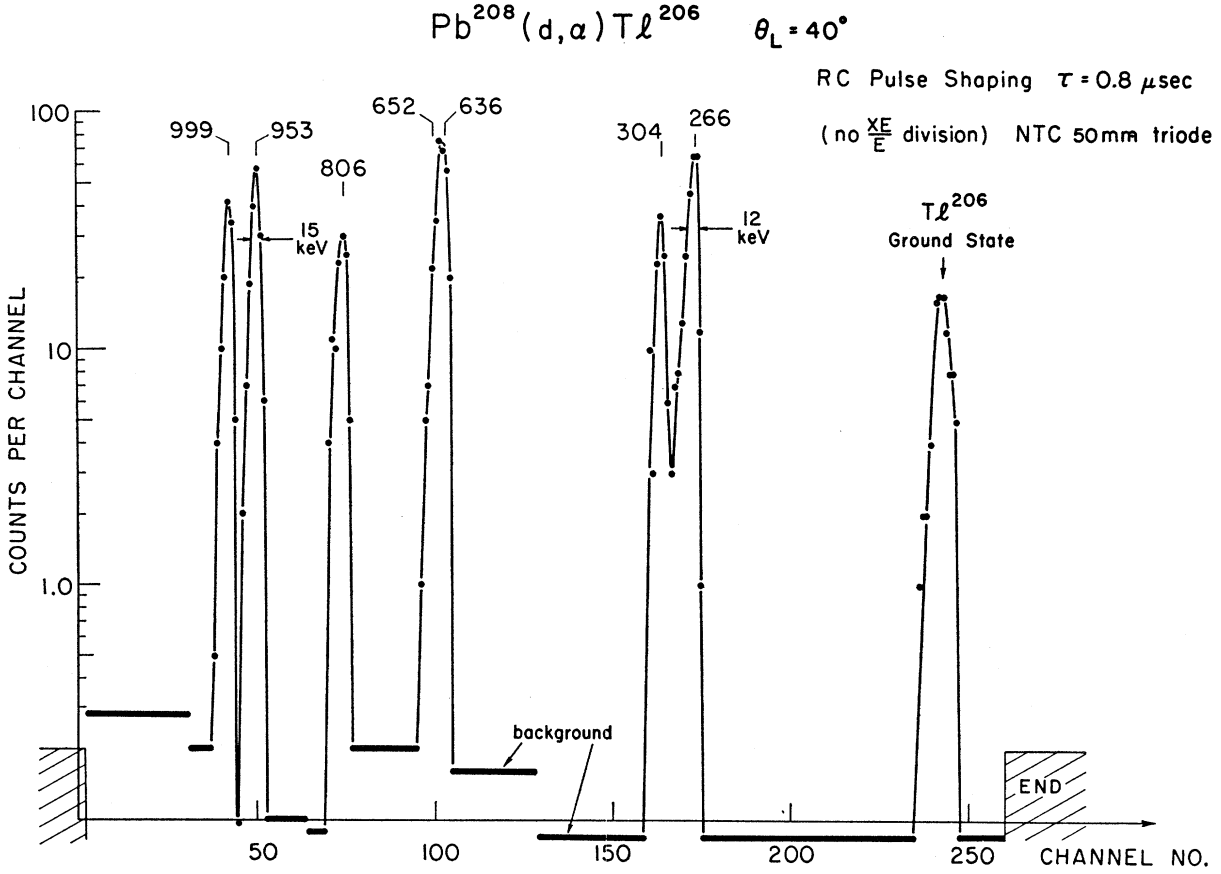

FIG. 1. Typical α spectrum observed with a single 50-mm-long position-sensitive detector at $\theta_L = 40°$. The energy of the α particles was about 28 MeV. Three or four such detectors (obtained from Nuclear Diodes, Inc.) were used to take the bulk of the data. The very low background after particle discrimination was averaged over the channels shown.

figuration amplitudes, including their phase. In addition, the angular distributions reveal the parity and limit the possible spin values of the final states.[2,3]

In previous studies, the ground state of Tl^{206} has been investigated by its β^- decay[4] to Pb^{206}. In addition, a few low-lying excited states have been seen in the radioactive α decay of the Bi^{210} isomer,[5,6] and more recently in neutron-capture studies.[7] Measurements of the ensuing γ rays and internally converted electrons have helped to limit the spin values of several levels. Single-particle transfer-reaction studies have also added to the understanding of the low-lying levels. For the $Tl^{205}(d, p)Tl^{206}$ reaction,[8] the neutron vacancy for stripping is assumed to be similar to that of Pb^{206}, so that presumably those $\pi^{-1}\nu^{-1}$ levels of Tl^{206} will be reached which contain appreciable $(3s_{1/2}{}^{\pi}3p_{1/2}{}^{\nu})^{-1}$ and $(3s_{1/2}{}^{\pi}2f_{5/2}{}^{\nu})^{-1}$ configuration admixtures. On the other hand, some deviation from this simple view is already evident from the splitting of the $3s_{1/2}$ hole strength seen in proton-transfer reactions,[9] and one cannot expect to interpret the intensities in (d, p) without difficulty. As Coulomb barrier effects in the 12-MeV (d, p) data of Ref. 8 tended to make angular distributions less distinct, we made supplementary measurements at 15° and 55° at 17 MeV for Pb^{206} and Tl^{205} to check on l_n transfers populating the low-lying two-hole states.

In the $Pb^{207}(t, \alpha)Tl^{206}$ study,[10] a pure $3p_{1/2}{}^{-1}$ configuration of the ground state of Pb^{207} is assumed as well established. This reaction should populate all Tl^{206} levels with an appreciable $(nlj)^{-1}3p_{1/2}{}^{-1}$ component, and the (t, α) cross sections greatly help to define the magnitude of these particular configuration amplitudes. However,

[2] N. K. Glendenning, Ann. Rev. Nucl. Sci. **13,** 191 (1963); Phys. Rev. **137,** B102 (1965).
[3] W. W. Daehnick and Y. S. Park, Phys. Rev. Letters **20,** 110 (1968); Phys. Rev. **180,** 1062 (1969).
[4] D. Alburger and G. Friedlander, Phys. Rev. **82,** 977 (1951).
[5] L. I. Rusinov, Yu. N. Andreev, S. V. Golenetskii, M. I. Kislov, and Yu. I. Filimonov, Zh. Eksperim. i Teor. Fiz. **40,** 1007 (1961) [English transl.: Soviet Phys.—JETP **13,** 707 (1961)].
[6] E. H. Spejewski, Nucl. Phys. **A100,** 236 (1967).
[7] C. C. Weitkamp, J. A. Harvey, G. G. Slaughter, and E. C. Campbell, Bull. Am. Phys. Soc. **12,** 922 (1967); J. A. Harvey (private communications).
[8] J. R. Erskine, Phys. Rev. **138,** B851 (1965).
[9] O. Nathan, G. Bruce, A. Bussierne, P. Kossanyi, J. M. Loiseaux, P. Roussel, J. Testoni, and L. Valentin, Nucl. Phys. **A109,** 481 (1968).
[10] P. D. Barnes, E. R. Flynn, G. J. Igo, and D. D. Armstrong (to be published).

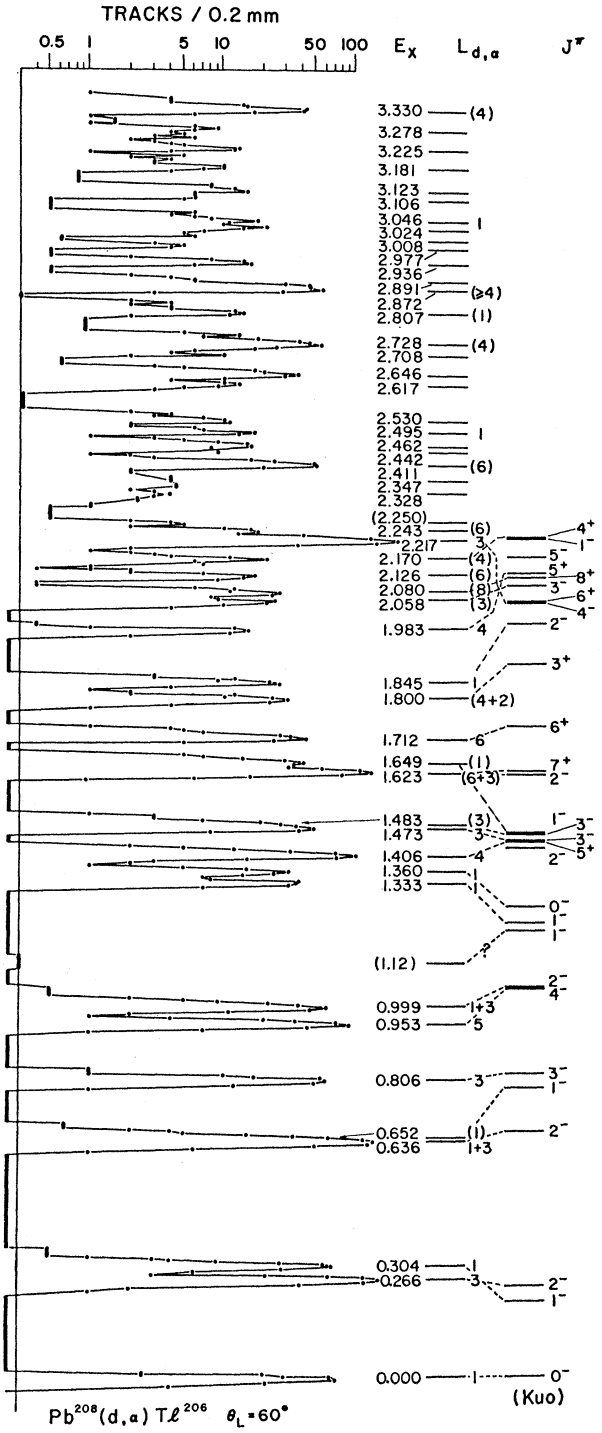

FIG. 2. A correlation of data and extracted L values with a theoretical spectrum calculated by Kuo. The spectrum shown here was observed with α-sensitive photographic emulsions in the focal plane of the split-pole Enge spectrograph at $E_d=17$ MeV and $\theta_L=60°$.

with (t, α) transfers one investigates only a fraction of the configuration space available to each level and, of course, the phases of the amplitudes do not play a role in the single-nucleon-transfer studies.

This work is intended to be a fuller account of work reported in a previous letter on the $Pb^{208}(d, \alpha)Tl^{206}$ reaction.[11] Where conflicts occur between the earlier report and this one, the latter represents the final conclusion of the authors.

II. EXPERIMENTAL PROCEDURE

Films of about 150 μg/cm^2 thickness were prepared by evaporation of 99.5% enriched metallic Pb^{208} onto 10-μg/cm^2 carbon foils. The foils were mounted on target frames with a 0.5-in.-high by 0.25-in.-wide aperture. Targets were checked for uniformity and thickness by exposing them to a deuteron beam at 11.8 MeV, and by measuring the peak shape and cross sections for elastic scattering with a position-sensitive detector mounted in an Enge split-pole spectrograph, with the spectrograph entrance aperture set at the same value as that used in the (d, α) reaction study, namely, $\Omega=1.4\times10^{-3}$ sr. The thickness could then be computed by comparing the elastic counts/charge collected with known cross-section measurements[12] in the 20°–90° region.

The $Pb^{208}(d, \alpha)Tl^{206}$ reaction was investigated with a deuteron beam energy of 17.0 MeV. Beam currents from the University of Pittsburgh three-stage tandem Van de Graaff were held to $\lesssim0.3$ μA in order to avoid deterioration of the Pb target. The beam energy spread was $\Delta E\approx2$ keV. A quadrupole lens positioned 106 cm upstream from the target produced a beam spot of about 0.5 mm in width and 2 mm in height, with a horizontal divergence of about 12×10^{-3} rad. The target colimating slit was positioned about 1 cm before the target and was followed by an antiscattering slit. More detailed descriptions of experimental setup and counting procedure have been given previously.[13,14]

The reaction α particles were detected by an array of three or four position-sensitive counters mounted in an Enge split-pole spectrograph. Each detector has a sensitive region 8 mm high and 50 mm in length. The gaps between successive detectors, corresponded to energy regions of about 200 keV. In order to obtain complete spectra, runs with two slightly different magnetic field settings were taken for each angle. The typical total experimental resolution with position counters was ~14 keV full width at half-maximum (FWHM) for the 28-MeV α particles observed in this work. Figure 1 shows a typical pulse height (XE) spectrum for α's observed in the first counter. It can be seen that the

[11] M. B. Lewis and W. W. Daehnick, Phys. Rev. Letters **22**, 77 (1969).
[12] G. Mairle and U. Schmidt-Rohr, Max Plank Institute für Kernphysik (Heidelberg) Report No. 1965 IV 113 (unpublished).
[13] W. W. Daehnick, Phys. Rev. **177**, 1763 (1969).
[14] M. B. Lewis, Phys. Rev. **184**, 1081 (1969).

TABLE I. A tabulation of Tl^{206} levels reached by (d, α), (t, α), (d, p), and (n, γ) reactions. The three right-hand columns are, respectively, the peak (d, α) cross section, the L transfer observed in $Pb^{208}(d, \alpha)Tl^{206}$, and the suggested spin parity based in part upon a comparison with shell model wave functions (see text).

Level	$E(d, \alpha)$ MeV	$E(t, \alpha)$[10] MeV	$E(d, p)$ MeV	$E(n, \gamma)$[7] MeV	σ_{max} (d, α) μb/sr	$L_{d,\alpha}$	J^π
0	0.000	0.000	0.000	0.000	17	1	0^-
1	0.266	0.273	0.263	0.266	58	3	2^-
2	0.304	0.303	0.305	0.305	19	1	1^-
3	0.636	···	0.635	0.635	40	1+3	2^-
4	0.652	0.647	0.650	0.650	(10)	(1)	1^-
5	0.806	0.806	0.802	0.802	23	3	3^-
6	0.953	···	···	(0.940)	21	5	4^-
7	0.999	1.002	0.998	0.998	23	1+3	2^-
				1.080			
8	(1.12)	1.121	1.117	1.117	<0.5	···	$(1^-, 2^-)$
				(1.205)			
9	1.333	(1.345)	1.335	···	13	1	$1^-(2^-, 0^-)$
10	1.360		(1.350)	1.361	7	1	$0^-(1^-2^-)$
11	1.406	1.409	···	···	50	(4)	5^+
				(1.453)			
12	1.473	···	···	···	25	(3, 4)	(3^-)
13	1.483	1.485			(10)	?	(3^-)
14	···			1.490	not res.	?	(2^-1^-)
15	1.623	···	···	···	(27)	(6)	(7^+)
16	(1.63)			(1.631)	(18)	(3)	(2^-)
17	1.649	1.653	···	···	(10)	(1)	(1^-)
18	1.712	1.717	···	···	14	6	6^+
19	1.800	···	···	···	15	(4+2)	(3^+)
20	1.845	1.852	···	(1.842)	9	1	2^-
21	1.983	1.985	···	···	5	4(3)	(5^+)
				(1.993)			
22	2.058	2.061	···	···	10	(3)	$3^-(2^-)$
23	2.080	···	···	···	6	(8)	(8^+)
24	2.126	2.128	···	···	(5)	(6, 1)	$(5^+, 6^+)$
25	2.170	···	···	···	(5)	(4, 3)	
26	2.217	···	···	···	65	3	4^-
27	2.243	···	···	···	6	(6)	
28	(2.25)	2.264	···	···	(2)	···	
29	2.328	···	···	···	(2)	···	
30	2.347	···	···	···	(2)	···	
31	2.411	···	···	···	13	(6)	
32	2.442	···	···	···	(2)	···	
33	2.462	2.464	···	···	(5)	···	
34	2.495		···	···	3	1	$(1^-, 2^-)$
		2.506					
35	2.530		···	···	4	(3, 4)	
			2.581				$(5^+, 4^+)$
			2.594				$(5^+, 4^+)$
36	2.617		···	···	8	(4)	
37	2.646	···	···		19	(4)	
38	2.708		···	···	(3)	···	
		2.717					

TABLE I. (*Continued*).

Level	$E(d,\alpha)$ MeV	$E(t,\alpha)$[10] MeV	$E(d,p)$ MeV	$E(n,\gamma)$[7] MeV	σ_{max} (d,α) μb/sr	$L_{d,\alpha}$	J^π
39	2.728		...	...	17		
40	2.807	2.813	...	...	5	(1)	
			2.828				
41	2.872	...	2.868	...	(19)	4	
42	2.891	...	2.896	...	(2)	...	
43	2.936	...	...	...	4	(6)	
44	2.977	...	...	...	(2)	...	
45	3.008		3.014	...	(2)	...	
46	3.024	3.022	...	...	7	(4, 3)	
47	3.046	...	...	...	3	1	$0^-, 1^-, 2^-$
48	3.106	...	...	...	(2)	...	
49	3.123	...	...	...	(2)	...	
50	3.181	...	...	...	(5)	...	
51	3.225	...	...	...	(7)	...	
52*	3.278	...	...	...	(5)	...	
53	3.330	...	...	...	20	(4)	

peak-to-background ratio was generally $\sim 10^3$. Also observable is a detector-dependent energy (XE) nonlinearity of about 8%. (The other detectors used were better in this respect.) This nonlinearity and statistics lead to slightly different values for the resolution, as shown.

In order to obtain more reliable energy assignments for many of the unknown levels, several runs (at 40°, 60°, and 70°) were also taken with α-sensitive photographic plates (50-μ Ilford K-1). An example of a complete plate spectrum is included in Fig. 2. Position-counter and plate resolutions were practically identical in this experiment, an indication that the major contributions come from the target thickness and target nonuniformity (estimated at 10 keV) and that the triode position resolution was significantly better than 1%.

Data were taken in 5° steps from 10° to 90° with an additional point at 12°. For the 10° and 12° runs, the collimating slit was increased to 1 mm. Typically, about 20000 μC of charge were collected for forward angles, while about 4000 μC were collected for the larger angles. We found that all α groups which have reasonable intensity and can be resolved, lie below 4-MeV excitation and occupy a region of $\lesssim 15$ cm along the focal plane. Hence, the use of three position counters was sufficient to examine the reaction products.

Relative cross-section measurements were made for the $Tl^{205}(d,p)Tl^{206}$ and $Pb^{206}(d,p)Pb^{207}$ reactions at 15° and 55° with the 17-MeV incident beam. Protons were detected with 25-μ Kodak NTB photographic plates. Beam optics and target geometry were again as described above.

III. EXPERIMENTAL RESULTS

A. $Pb^{208}(d,\alpha)Tl^{206}$ Reaction

It is evident from Fig. 2 that the level density of Tl^{206} is larger than that suggested by previous[5–9] experiments. Nevertheless, we believe that in the 3-MeV energy interval shown only a few $\pi^{-1}\nu^{-1}$ states have gone unnoticed because of limited detection resolution. We generally find the more strongly excited states at lower excitation. In the high-excitation-energy region, most states are unresolved and have about 1/20 the magnitude of the ground state. As will be shown below, this decrease of the cross section is not simply a Coulomb-barrier effect but also a $\pi\nu$ correlation effect. A listing of the observed levels is given in Table I. Levels energies based on the (d,α) experiment have an uncertainty of about 0.3% of excitation energy.

The angular distributions of the reaction products shown in Fig. 3 display considerable structure, although somewhat less than that seen in lower-mass regions.[3,14] (This is expected in part from the influence of the Coulomb barrier in the α channel.) The angular distributions showed recurring patterns and have been grouped accordingly. Usually, L values could be assigned with the aid of the distorted-wave reaction analysis discussed in Sec. IV. Statistical errors and, sometimes, resolution problems are primarily responsible for the error bars shown in Fig. 3. The absolute cross-

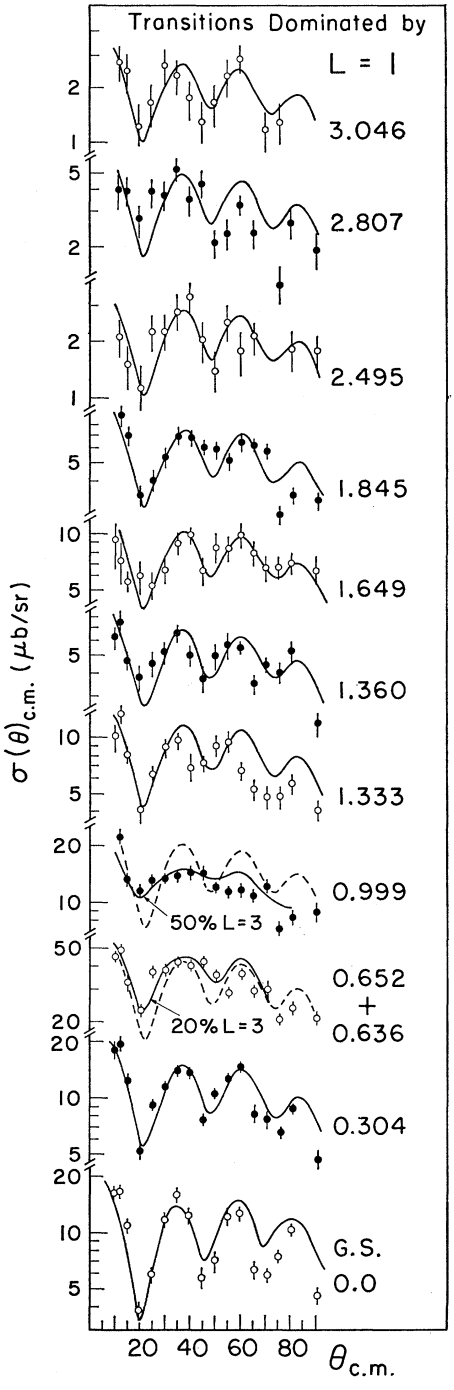

(a)

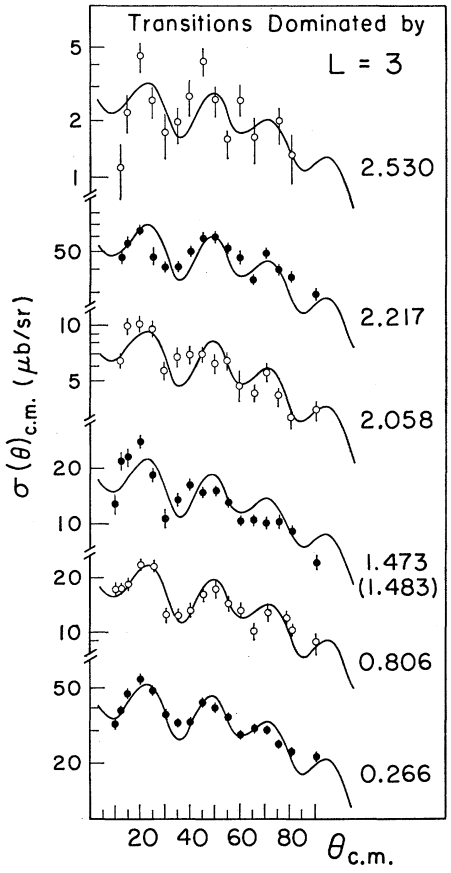

(b)

FIG. 3. Experimental cross sections and DWBA calculations grouped according to L transfer. The experimental absolute scale error is about 15 %. The DWBA cross-section calculations are shown by solid lines and are arbitrarily normalized to the data and discussed in the text. The dotted lines are empirical curves for larger L values.

section scale error arises primarily from uncertainties in the elastic cross section and in charge collection, and is estimated at ±15%.

B. $Tl^{205}(d, p)Tl^{206}$ Reaction

A typical experimental spectrum from the $Tl^{205}(d, p)Tl^{206}$ reaction of $E_d=17$ MeV is shown in Fig. 4. Below 2.5-MeV excitation, only a few $\pi^{-1}\nu^{-1}$ states are populated. Above 2.5 MeV, strong one-particle–three-hole states appear. Only one new level at 1.360 MeV was seen which had not been reported for the 12-MeV experiment of Ref. 8. However, we find considerable variations in the 15°–55° cross-section ratio. By comparison with the $Pb^{206}(d, p)Pb^{207}$ reaction at the same angles and energy it is possible to discriminate between $3p$ and $2f$ neutron capture. The cross-section ratios of the 15°–55° data for the $3p_{1/2}$, $3p_{3/2}$, and $2f_{5/2}$ states well known in Pb^{207} were found to be 1.40±0.08, 1.80±0.2, and 0.57±0.09, respectively. The ratios found for $Tl^{205}(d, p)Tl^{206}$ reaction are given in Table II along with the deduced l transfer.

IV. (d, α) REACTION ANALYSIS

A. DWBA Formalism

In our analysis of the reaction mechanism, we assume a direct deuteron pickup process and follow a formalism similar to that of Glendenning,[2] except that our treatment of the deuteron form factor is that of

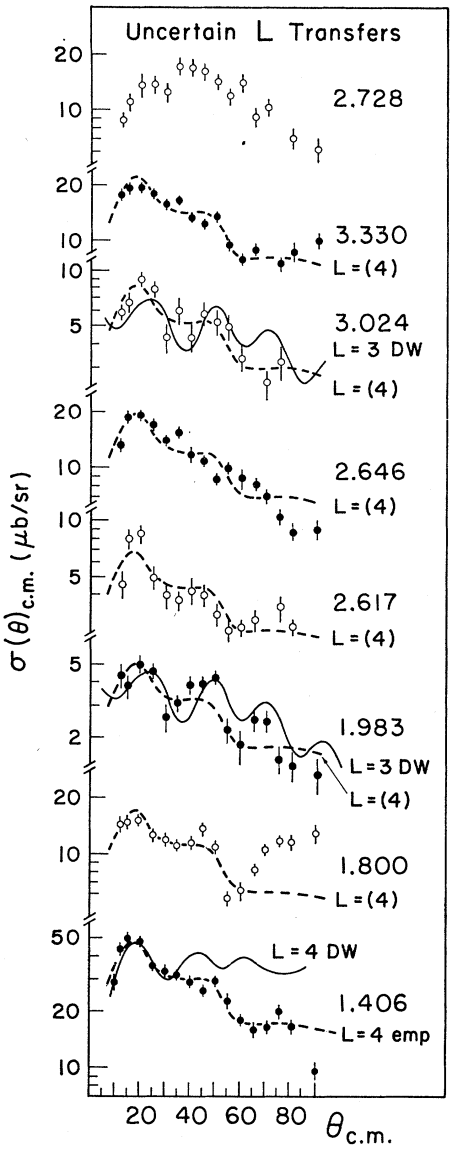

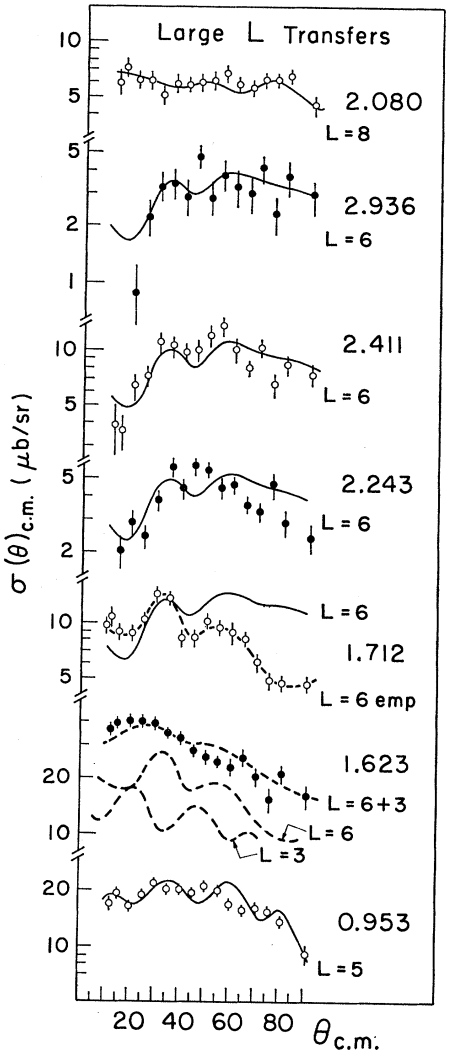

FIG. 3. (*Continued*).

Drisko and Rybicki.[15] Successful applications of (d, α) transfer calculations to the spectroscopy of odd-odd nuclei can already be found in Refs. 3 and 14. In this treatment we expand the DWBA analysis discussed in Ref. 3 to make use of explicit $\pi^{-1}\nu^{-1}$ Tl^{206} shell-model wave functions, obtained and made available to us by Kuo.

The zero-range DWBA treatment of the one-step pickup of a two-nucleon cluster with given L, S, J, and T leads to the cross section

$$d\sigma/d\Omega \sim N \sum_M |\int \psi^{(-)*} F_{LSJT}(R)\, Y_L^M(R) \psi^{(+)} d^3R\,|^2, \quad (1)$$

where the form factor F is a radial function, derived from an expansion in terms of its explicit parentage

$$F_{LSJT}(R) = \sum_\gamma \beta_{\gamma LSJT} f_{L_\gamma}(r),$$

with

$$f_{L_\gamma}(R) = \sum_N g_{NL_\gamma} U_{NL_\gamma}(R). \quad (2)$$

The quantum numbers L, S, J, and T refer to orbital angular momentum, spin, total angular momentum, and isotopic spin, respectively, of the transferred pair and in this special case of a doubly magic target (Pb^{208}), L, S, and J refer to the two-hole configuration as well.

The values of R and N refer to the c.m. motion of the proton-neutron "cluster" while γ refers to one of the $[j_1 j_2]_J$ nucleon pair configurations that contribute to the reaction. The value of $\beta_{\gamma LSJT}$ is then the spectro-

[15] R. M. Drisko and F. Rybicki, Phys. Rev. Letters **16**, 275 (1966). The authors are indebted to Dr. Drisko and Dr. Rybicki for the use of their microscopic-form-factor code MIFF.

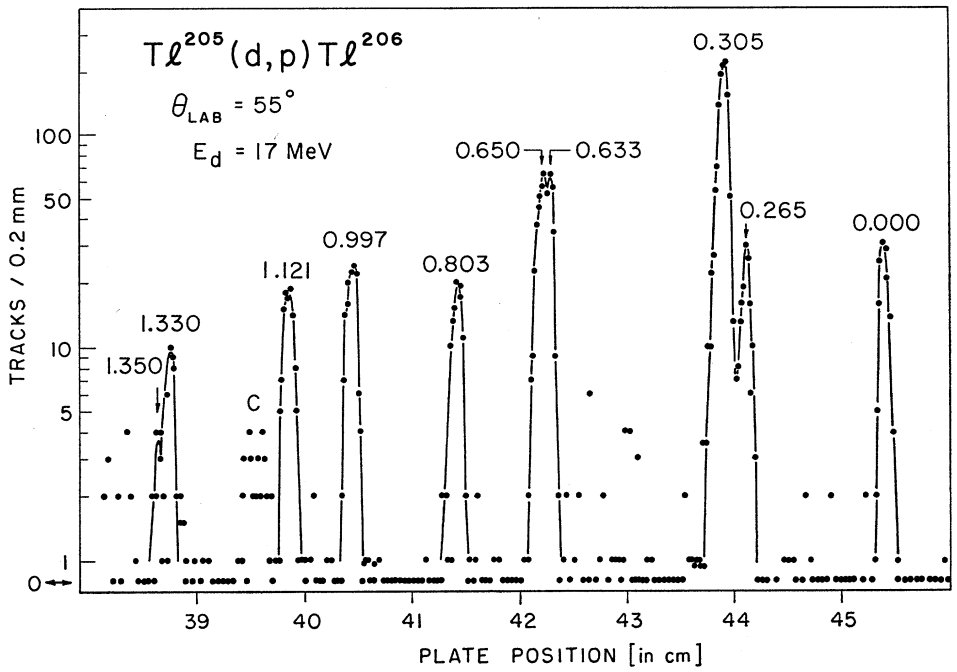

FIG. 4. A typical $Tl^{205}(d, p)Tl^{206}$ spectrum at 55° and $E_d=17$ MeV, taken with photographic emulsions. The energies (in MeV) are those measured for this (d, p) run.

scopic amplitude for this configuration γ, while $U_{NL_\gamma}(R)$ is a component of the two-nucleon radial wave function[2] and g_{NL_γ} is defined[3] as the product of a symmetry factor g (here=1), an overlap integral Ω_n, and a Moshinsky bracket:

$$g_{NL_\gamma}=g\Omega_n\langle n0, NL, L \mid n_1l_1, n_2l_2, L\rangle. \quad (3)$$

It is clear that aside from the treatment of the form factor we may proceed as in the case of single-nucleon transfer reactions and carry out computations of relative cross section using standard DWBA codes. In this work, we employ code DWUCK[16] and include finite-range and nonlocality corrections, but ignore any possible effects of the deuteron spin-orbit potential. The separately generated microscopic form factor $F_{LSJT}(R)$ (discussed below) is read into the code (externally) via data cards.

An understanding of the expected absolute cross section is important in the analysis of transition strengths. Analogous to the case of single-nucleon transfer reactions, N in Eq. (1) depends on the type of transfer reaction studied not on the particular target; or in other words, on the intrinsic structure of the nuclear clusters in the reaction channels.

Once N is determined for the (d, α) or (α, d) reaction, we can express the (d, α) cross section as

$$\frac{d\sigma}{d\Omega}(\text{mb/sr})=N(d,\alpha)\left(\frac{(2S+1)}{2}\frac{\sigma_{\text{DWUCK}}(\text{mb/sr})}{2J+1}\right), \quad (4)$$

where

$$N(d, \alpha)=(2S_\alpha+1)N(\alpha, d)/(2S_d+1)$$

{In code JULIE, the statistical factor

$$[(2S+1)/2][1/(2J+1)]$$

is absorbed in the program and need not be considered explicitly.}

B. Microscopic Form Factor

The radial form factor terms $f_{L_\gamma}(R)$ in Eq. (2) were computed with code MIFF. With this code, single-

TABLE II. Comparison of $Pb^{206}(d, p)Pb^{207}$ and $Tl^{205}(d, p)Tl^{206}$ reactions. The three columns are, respectively, the excitation of the final state, ratio of 15°–55° cross sections, and probable nlj transfer.

Nucleus	Excitation	Ratio σ_{15}/σ_{55}	nlj
Pb^{207}	0.000	1.40±0.08	$3p_{1/2}$
	0.570	0.57±0.09	$2f_{5/2}$
	0.897	1.80±0.2	$3p_{3/2}$
Tl^{206}	0.000	1.6±0.2	$3p$
	0.265	1.1±0.2	$(3p+3f)$
	0.305	1.38±0.08	$3p$
	0.633	1.30±0.1	$3p(+3f)$
	0.650		
	0.803	0.80±0.14	$(3f)$
	0.997	0.40±0.1	$(3f)$
	1.121	0.50±0.1	$(3f)$

[16] DWBA code DWUCK and instructions by P. D. Kunz (unpublished). The authors are indebted to P. D. Kunz for making available this code. Our finite-range corrections utilized the correct α-d separation energy, normally not listed in code DWUCK.

TABLE III. Optical-model parameters used for the deuteron and α channels in standard notation.

Channel	V_0 (MeV)	r_0 (fm)	a (fm)	r_c (fm)	W (MeV)	$4W'$ (MeV)	r_I (fm)	a_I (fm)
d	93.4	0.986	1.184	0.986	0	49.6	1.484	0.621
α III	177.3	1.342	0.569	1.30	15.6	0	1.342	0.569
α II	124.7	1.380	0.566	1.30	10.0	0	1.380	0.566
α I	58.8	1.454	0.560	1.30	5.83	0	1.454	0.560

nucleon Woods-Saxon radial wave functions were generated, with their correct asymptotic form assured by the usual well-depth search technique. The configurations considered were $3p_{1/2}$, $2f_{5/2}$, $3p_{3/2}$, $i_{13/2}$, or $2f_{7/2}$ for neutrons, and $3s_{1/2}$, $2d_{3/2}$, $h_{11/2}$, $2d_{5/2}$, and $g_{7/2}$ for protons. Each nucleon wave function was expanded in a seven-term harmonic-oscillator series, while a ten-term series was used to represent the "deuteron." In this way, one can produce the bound "deuteron wave function" by transforming the product of the neutron and proton finite-well expansions $\phi_{n_1l_1}(r_1)$ and $\phi_{n_2l_2}(r_2)$ into a product of their relative $[\Phi(r)]$ and c.m. $[U(R)]$ motions, as described earlier.[2,3,15] Equation (5) shows the relation of $\Phi(r)$ and $U(R)$ to the coupled single-particle wave functions:

$$[\phi_{n_1l_1}(r_1)\phi_{n_1l_1}(r_2)]_L=\sum_{nN}\langle n0, NL; L \mid n_1l_1n_2l_2, L\rangle \times[\phi_{n0}(r)\,U_{NL}(R)]_L. \quad (5)$$

The expression for the spectroscopic amplitudes β relating the 0^+ ground state of Pb^{208} to a final state J^π in Tl^{206} takes a simple form due to the double-shell closure of Pb^{208} and becomes[2]

$$\beta^{0J}{}_{\gamma LSJT}=C_\gamma(2J+1)^{1/2}\begin{bmatrix} l_1 & \frac{1}{2} & j_1 \\ l_2 & \frac{1}{2} & j_2 \\ L & S & J \end{bmatrix}\delta_{T,0}, \quad (6)$$

where the square bracket is the LS-JJ transformation coefficient. The C_γ are the normalized shell-model amplitudes representing the strength of the $[j_1^{-1}j_2^{-1}]_J$ configuration in the final state of Tl^{206}. It is clear from Eqs. (1), (2), and (6) that the phases as well as magnitudes of the configuration amplitudes affect the (d, α) cross section.

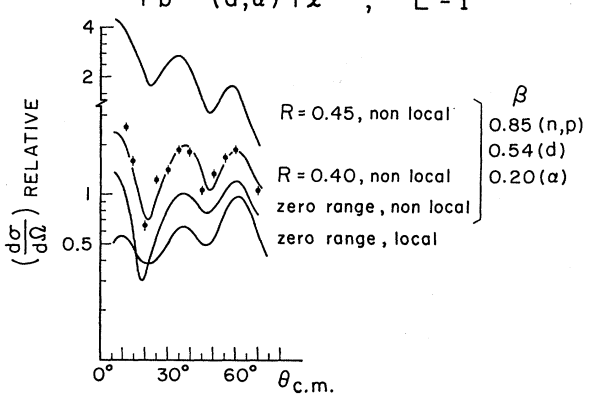

FIG. 5. The effect of finite-range and nonlocality parameters on the predicted $L=1$ cross section for $Pb^{208}(d, \alpha)Tl^{206}$.

C. Relative Cross Section

Computations were carried out both with "cluster"[3] and microscopic[15] form factors. The optical-model parameters used[17,18] are given in Table III. Nonlocality parameters of $\beta_d=0.54$ and $\beta_\alpha=0.2$ were used for the elastic scattering channels. We find that at forward angles the $L=1$ transfers are affected by the finite-range and nonlocality corrections (see Fig. 5) and that empirically a value of $R_{d,\alpha}=(0.38$–$0.42)$ as defined for DWUCK[16] is preferred. Thus the value of 0.4 used in this work is the same as in previous (d, α) studies.[3,14] (Note that the parameter R is defined differently by various authors, e.g., frequently as twice the quantity used in DWUCK[19]) Although radial cutoffs were not used in this work, their effect on the cross sections was investigated to study the importance of contributions from the nuclear interior. Figure 6 illustrates the interior contributions to a typical $L=3$ transfer for three reaction angles. The forward-angle cross sections are appreciably effected by the deep interior of the nucleus even when finite-range and nonlocality corrections are made.

The importance of contributions from the nuclear interior is also evident from the sensitivity of DWBA predictions to the optical scattering parameters. As in previous (d, α) studies, the choice of the correct optical-model parameter family for the elastic α channel (roughly four times single-particle well) was crucial for good agreement with experiment. Of the "equivalent" sets of α parameters[18] shown in Table III only set III predicted relative cross sections in agreement with experiment. The shallower wells lead to completely different predictions as illustrated for a typical $L=3$ transition in Fig. 7. Note that the shape as well as absolute magnitude and structure change with the α family used.

Microscopic form factors $f_{L\gamma}(R)$ were calculated for many configurations γ. The results confirmed that within a harmonic-oscillator shell the shape of $f(R)$ was

[17] C. M. Perey and F. G. Perey, Phys. Rev. **132**, 755 (1963).
[18] L. McFadden and G. R. Satchler, Nucl. Phys. **84**, 177 (1966).
[19] See, for instance, R. Bassel, Phys. Rev. **149**, 791 (1966).

TABLE IV. Form-factor analysis for two 3^- shell-model states illustrating the typical effects of configuration mixing (see text for details).

Configuration	$C_\gamma^{(20)}$	$[jj\text{-}LS]$	Microscopic form factor at $R_N=7$ fm	Approximate amplitude at R_N
$J^\pi=3^-$, 0.81 MeV				
$s_{1/2}f_{5/2}$	0.898	0.756	1.53	+1.04
$s_{1/2}f_{7/2}$	−0.109	−0.655	1.50	+0.11
$d_{3/2}p_{3/2}$	0.252	0.730	1.88	+0.35
$d_{3/2}f_{7/2}$	0.108	0.655	1.60	+0.12
$d_{5/2}p_{1/2}$	0.251	0.667	1.90	+0.31
$d_{5/2}f_{5/2}$	0.175	0.717	1.60	+0.20
				2.13 (sum)
$J^\pi=3^-$, 2.09 MeV				
$s_{1/2}f_{5/2}$	−0.138	0.756	1.53	−0.16
$s_{1/2}f_{7/2}$	0.138	−0.655	1.50	−0.14
$d_{3/2}p_{3/2}$	−0.305	0.730	1.88	−0.42
$d_{5/2}$, $p_{1/2}$	0.925	0.667	1.90	1.17
$d_{5/2}f_{5/2}$	−0.076	0.717	1.60	−0.09
				+0.36 (sum)

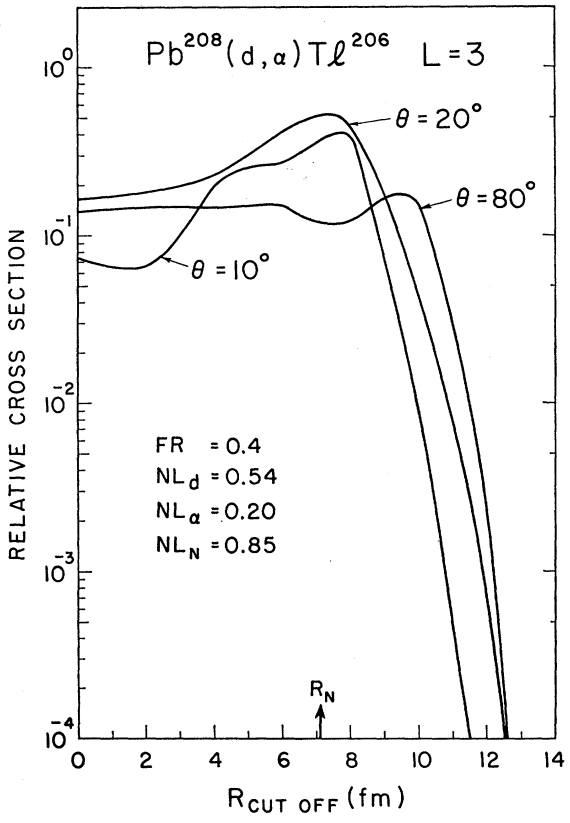

FIG. 6. The calculated cross sections for $L=3$ transfer at three angles 10°, 20°, and 80° are plotted as a function of radial integration cutoff, in order to illustrate importance of contributions from the nuclear interior, even when finite-range and nonlocality corrections (as listed) are included.

determined almost exclusively by the L value; i.e., it was otherwise nearly independent of the constituent neutron and proton orbitals. When a configuration dependence did appear, differences in the shape of $f_{L_\gamma}(R)$ occurred deep in the nuclear interior rather than near the surface, although the magnitude of $f_{L_\gamma}(R)$ varied by as much as a factor of 2 for various choices of

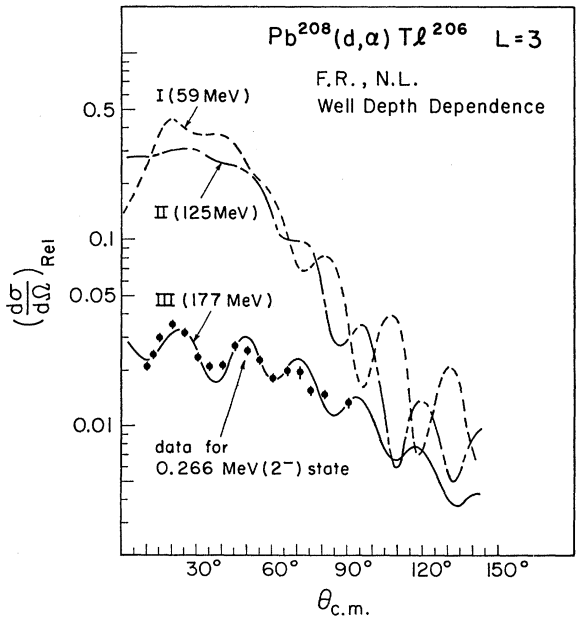

FIG. 7. Comparison of $L=3$ calculations obtained with different parameter families with experiment. Note that the same "family" (I), that was preferred for lighter elements (Ref. 3), produces best agreement with the data.

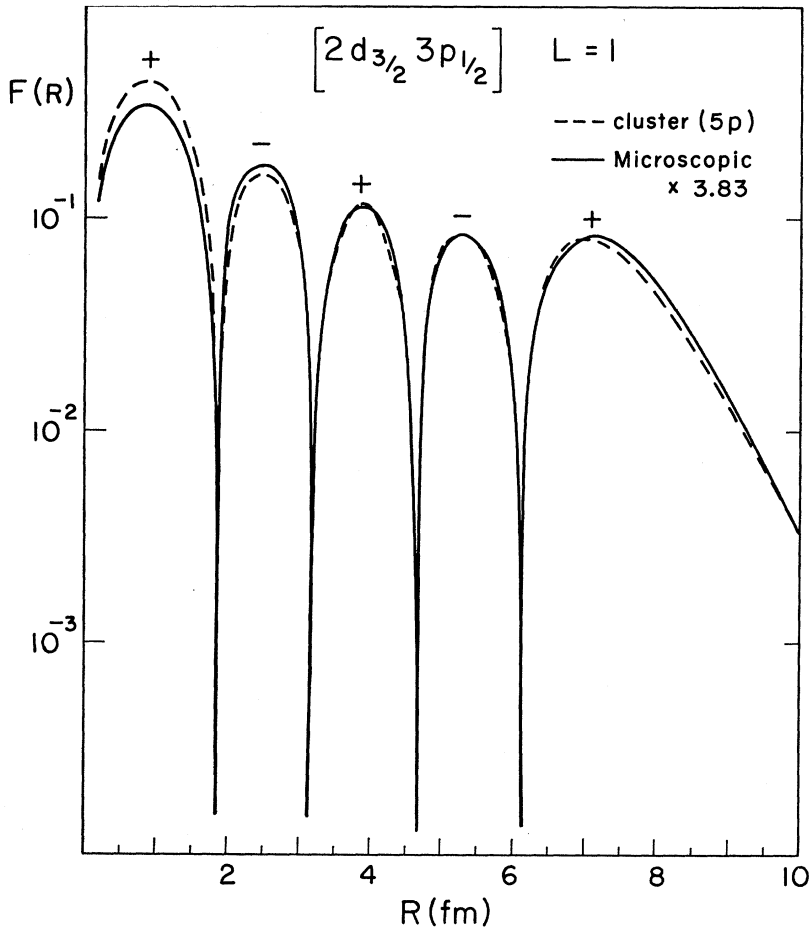

FIG. 8. Comparison of a microscopic $[2d_{3,2}3p_{1/2}]_{L=1}$ form factor with a $5p$ deuteron cluster fit for a realistic bound-state well geometry. The cluster has the correct asymptotic behavior given by the deuteron separation energy.

γ. Usually, microscopic form factors were very similar to a simple mass-two cluster form factors with the proper quantum numbers and a suitably adjusted well geometry. An example of the close resemblance of such form factors is shown in Fig. 8. A few exceptions were noted for some configurations involving the $1h_{11/2}$ orbit.

The values of the *LS-JJ* transformation bracket in Eq. (4) are sensitive to both the configuration γ and to the L value. In Table IV, the major contributions for two form factors are presented to illustrate the importance of admixed configurations for the predicted cross section. The first column shows the major configurations for the two 3^- states predicted at 0.81 and 2.09 MeV followed by the configuration amplitudes C_γ from recent shell-model calculations of Kuo.[20] The third column contains the *LS-JJ* bracket value, while the fourth column represents the approximate magnitude and phase (consistent with the shell-model phase convention) of the form factor term $f_{L\gamma}(R=R_N)$ at the nuclear surface. For purposes of illustration the approximate transition-amplitude product is then given in the extreme right column. The coherent sum of the amplitudes is proportional to $F_{LSJT}/(2J+1)^{1/2}$ in Eq. (2). Since the reaction cross section for a given L is proportional to $F_L^2(R)$ the higher-lying 3^- state is expected to be at least an order of magnitude weaker than the lower 3^- state. It is clear that the configuration admixtures enhance the transition to the 0.81-MeV state while weakening that to the 2.09-MeV level. On the other hand, it can be seen that in the *absence* of admixtures, the 2.09-MeV level would have a slightly larger amplitude than that of the 0.81-MeV state.

Similar remarks are valid throughout the entire $Pb^{208}(d,\alpha)Tl^{206}$ spectrum, and may be summarized as follows:

(a) If the daughter states are grouped wtih respect to J^π, the lowest excited state is enhanced over all higher excited states of the same J^π. In case the state can be reached by two L transfers, only one L transfer is enhanced, but the next excited state is reached with enhancement of the other allowed L transfer.

(b) The enhanced states may be conceivably viewed as a collective "proton-neutron pairing vibrations" in

[20] The authors are indebted to T. T. S. Kuo for kindly sending us the results of his preliminary calculations of Tl^{206}. In these calculations, the Hamada-Johnston potential was used as a residual interaction to generate the $\pi^{-1}\nu^{-1}$ wave functions. A first-order core polarization correction was also included. Eleven single-hole orbitals, listed in Sec. IV B were used.

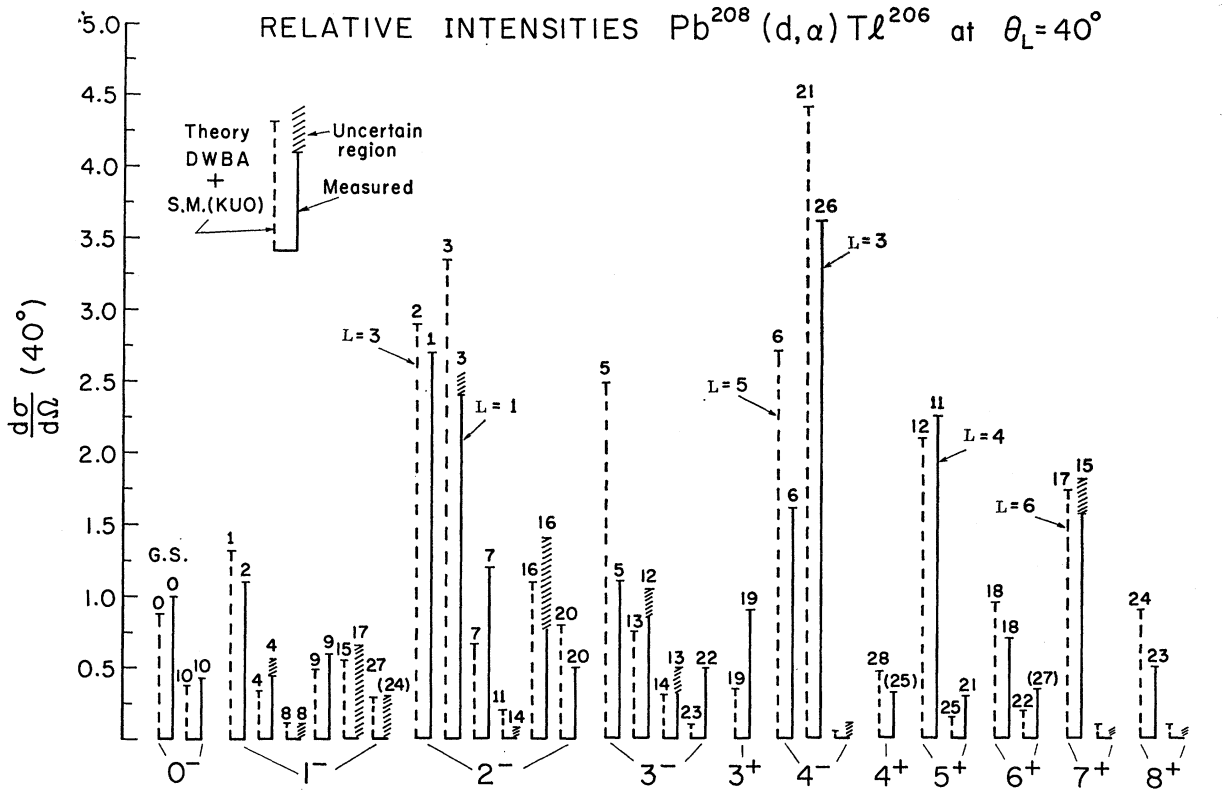

FIG. 9. Comparison of absolute experimental cross sections (taken at 40°) and microscopic DWBA calculations when explicit wave functions (Ref. 20) are considered and a normalization of $N(d, \alpha) = 20$ is applied (see text). Numbers above bars indicate experimental or theoretical level sequence. (Compare Fig. 2.)

the sense that the cross section to such states can be enhanced by as much as a factor of 5 over pure $\pi^{-1}\nu^{-1}$ configurations without admixtures. The transfer enhancement is a result of almost completely constructive (i.e., constant) phases in the constituent amplitudes throughout the π-ν configuration space ($Z = 50$–82, $N = 82$–126).

(c) Many of the higher-lying excited states are very weak owing to destructive coherence (i.e., oscillating phases). Thus, the use of a sum rule for a given J^π set of states may be practicable.

D. Absolute-Cross-Section Normalization

DWBA curves using cluster form factors are shown in Fig. 3 and are arbitrarily normalized. It appears that the data do not show any obvious configuration dependence in their angular distributions. However, configuration mixing does produce considerable intensity variations. In Fig. 9, experimental intensities at $\theta_L = 40°$ are shown by solid bars for groups of states of a given J^π. (The determination of J^π is discussed in Sec. V.) The adjacent, broken lines in Fig. 9 represent the direct predictions of the microscopic DWBA calculations discussed above, with a normalization[21] of $N(d, \alpha) = 20$ chosen to fit the entire spectrum in a "best average" manner.

A possibly more objective approach would be to assume (and this has been at least partially verified) that the form-factor shape for a particular L value is indeed configuration-independent, in which case a spectroscopic sum rule may be applied.[22] The logical J^π choice for this test would be the 0^- since there are only 4 such levels. The predicted 0^- strength of the two 0^- states omitted in Fig. 9 is only 14% of the total calculated strength. If we assume that this strength does reside in the spectrum, through unidentified, then the ratio of experimental/calculated strength yields

$$N(d, \alpha) = \sum \sigma_{\text{expt}} \Big(\sum \frac{2S+1}{2} \frac{\sigma_{DW}}{2J+1} \Big)^{-1} = 23.$$

Another possible normalization would be to give most weight to those shell-model states which are expected to have the purest configurations provided they agree closely with the spectroscopic measurement from the (t, α) reaction studies.[10] This would result in $N(d, \alpha) \simeq 17$.

Thus for the calculations of this study, $N(d, \alpha) \simeq 20$ appears to be a fairly consistent normalization which may aid us in further comparisons of shell-model-based

[21] The natural units of N are absorbed internally in the DWUCK (or JULIE) code.

[22] R. M. Drisko (private communication).

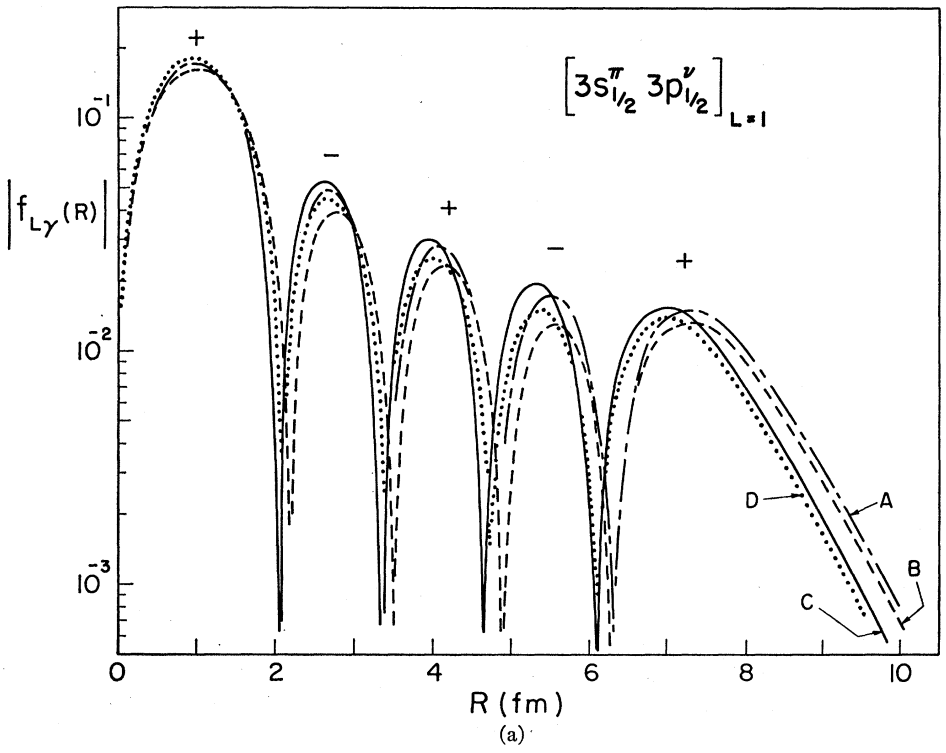

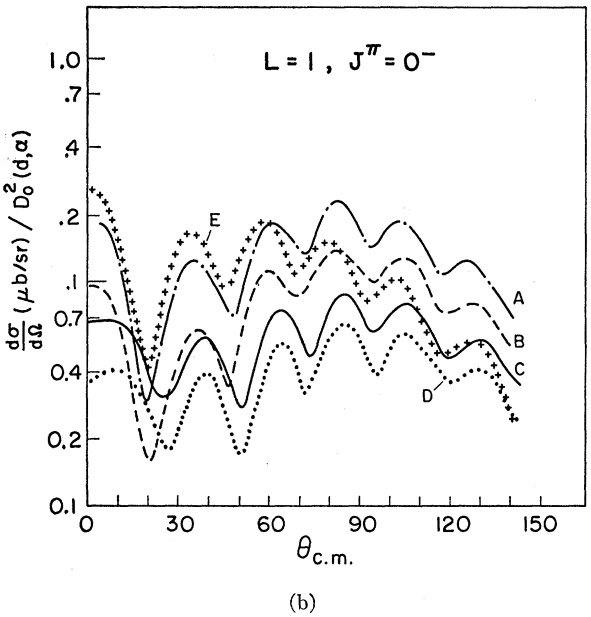

FIG. 10. Effect of different proton-well geometries and α size parameters (see text) on microscopic formfactors (a) and angular distributions for a pure $[s_{1/2}p_{1/2}]_{0^-}$ configuration (b). Figure 10(a) shows absolute values of four microscopic form factors that differ in the size parameter β for the α particle and in the proton-well geometry. Figure 10(b) shows the corresponding predictions for the angular distributions. Legend: A→large proton well ($r_0=1.35$, $a=0.85$), $\beta=0.35$; B→large proton well, $\beta=0.53$; C→small proton well ($r_0=1.25$, $a=0.65$), $\beta=0.35$; D→small proton well, $\beta=0.53$; E→prediction resulting from d-cluster form factor fitted to B with 94% overlap ($r_0=1.27$, $a=0.8$). Curve E gives best agreement with experiment.

DWBA and experimental values. It is clear from Fig. 9 that there is general qualitative agreement between theory and measurement. In particular, the predicted coherent enhancement for the states lowest in excitation in every $J^{\pi}(L)$ group has been seen experimentally. This suggests that we have the correct phases for the shell-model amplitudes. If the phases are indeed as predicted, then the "degree" of configuration mixing is given by the ratio of the strength of enhancement to nonenhanced states; and the ratio grows with an increasing percent of admixtures.

Our absolute normalization constant N for (d,α) transitions may not be of general validity as it depends on many calculational parameters, most of which are not uniquely fixed. To begin with, the magnitude of the structure terms g_{NL_γ} [Eq. (3)] depends on the value of Ω_n, which is the overlap integral for the relative motion of the transferred nucleons in the target with the motion of the pair in the free α particle. In the present form-factor calculations, the size parameter for the reaction α was somewhat arbitrarily chosen as $\beta=m_p\omega/h=0.35$. A more widely accepted choice would be[2] $\beta=0.43$ or[22] $\beta=0.53$. (The value $\beta=0.35$ implies a relative increase of the α-projectile radius of about 20% and tends to give better agreement with data as well as with the cluster form factors.) The decrease in β also tends to increase Ω_n; hence, our microscopic form factors, apart from small errors in their radial dependence, may be systematically 20–30% too large. (Compare Fig. 10.)

A second, marked effect on the absolute cross section comes from the use and choice of finite-range and non-

locality corrections. For $Pb^{208}(d, \alpha)$, the calculated absolute cross sections vary noticeably with the parameters β and R. Although the nonlocality parameters used $\beta(\text{nucleon})=0.85$, $\beta(\text{deuteron})=0.54$, and $\beta(\alpha)=0.20$ are based on theoretical considerations and have commonly been chosen by many investigators,[16] their values cannot be considered final[1] and others may be used in future work. The finite range parameter $R(d, \alpha)$ has not been investigated theoretically. The correct functional form of the correction factor $W(R)$ may, in fact, differ from that for single-nucleon transfers. Our empirical choice $R=0.4$ is based on the success of this value in Ref. 3 and because it also seemed to do best for the strongly structured $L=1$ transitions in $Pb(d, \alpha)$ (see Fig. 5). Setting $R=0$ results in a predicted (d, α) cross section smaller by nearly a factor of 2.

Absolute cross sections also depend strongly on the size and shape of the finite well used to generate the single-nucleon wave functions. We used a neutron well with the conventional parameters $r_0=1.25$ fm $(=r_c)$, $a=0.65$ fm, and $\lambda=25$. When the same potential geometry was used for protons, protons were found to have significantly smaller rms radii than neutrons of the same separation energy. In a $Pb^{208}(d, He^3)$ analysis,[1] such a conventional proton well yielded poor angular distributions and unrealistic spectroscopic factors (too large). There are good reasons why the bound-state proton potential might differ from the neutron well, especially in heavy nuclei. An obvious change in the desired direction would follow from the use of a $\mathbf{t}\cdot\mathbf{T}$ surface term for the well.[22] As these questions have not been answered theoretically, we preferred to use a trial proton well for Pb with $r_0=r_c=1.35$ fm, $a=0.85$ fm, and $\lambda=25$, which leads to more similar rms radii for the least bound neutrons and protons. Figure 10 illustrates the difference of form factors and angular distributions obtained with the "conventional" and "trial" proton wave functions for a pure $[3s_{1/2}3p_{3/2}]_{0^-}$ configuration. It is noted that the larger proton well increases the predicted cross section by almost a factor of 2, and leads to better agreement with experiment.

If these and other uncertainties inherent in our first attempt to empirically find N are considered it becomes clear that the proposed value remains uncertain to at least a factor of 2.

V. DISCUSSION OF INDIVIDUAL LEVELS AND CORRESPONDING SHELL-MODEL WAVE FUNCTIONS

Ideally, one would like to determine properties of nuclear levels by analyzing data with only such theories and theoretical arguments that are well established and generally accepted. Occasionally, as in γ-γ correlations or direct (p, t) transitions, for instance, the assignment of final-state J values is unique, because of the simple interpretation and selection rules for the experimental data. In direct (d, α) reactions we can reliably extract the level energies, their isospin T and, normally, the transfered angular momentum L. The L determination may become difficult if levels are poorly resolved, or two weakly structured L transitions contribute at the same time. The excitation of natural parity states reached by (d, α) from 0^+ targets must go by $L=J_f$, and many L transfers are sufficiently structured to permit reliable L and parity, $\Pi=(-1)^L$, assignments. However, the observation of an (apparently) pure-L transfer, in contrast to (p, t) work, does not prove that the final state has natural parity. Although in the majority of cases this is so, the strong selection rule merely requires $L-1\leq J_f\leq L+1$.

Additional experimental information, such as different, partially overlapping ranges for J_f (deduced from single-nucleon transfers or γ decay) may reduce the ambiguity and single out the correct J^π value. The danger in combining J_f ranges from different experiments is that sometimes different members of close doublets are excited by different experiments. Particularly where the level density is high or the resolution poor, this method looses reliability with increasing excitation energy. Nevertheless, for low-lying levels, the combination of results from different experiments is most valuable and often leads to unique assignments. In our discussion, we shall repeatedly refer to γ-transition studies (Refs. 4–7) and (t, α) results (Ref. 10) in support of particular assignments. Reference to (d, p) work includes our own study at 17 MeV and earlier work by Erskine[8] at 12 MeV.

Next to "strong" experimental selection rules we will often take recourse to model-dependent structure arguments or considerations of transition strengths. Since our target Pb^{208} is doubly magic and the daughter Tl^{206} only two nucleons removed, shell-model ideas as well as theoretically predicted wave functions should at least be consistent with our conclusions. As will be pointed out below, the experimental correspondence with Kuo's Tl^{206} two-hole wave functions generally is so good that often a detailed confirmation of admixtures and their signs seems possible.

Ground State, $E_x=0$

Shell-model cosiderations, which suggest $(3s_{1/2}{}^\pi 3p_{1/2}{}^\nu)^{-1}$ as the dominant configuration, have been confirmed by the observation of strong $l=1$, $Tl^{205}(d, p)$ and $l=0$, $Pb^{207}(t, \alpha)$ transitions.[8,10] This configuration can only couple to 0^- and 1^-. The pure $L=1$, $Pb^{208}(d, \alpha)$ transition independently set the limits $J^\pi=0^-$, $1^-(2^-)$. β decay to the Pb^{206} 0^+ ground state rather than the 2^+ (0.80-MeV) level, and γ-transition studies suggest $J=0$. The resulting assignment, $J^\pi=0^-$, is also in agreement with (d, p) and (t, α) spectroscopic factors. The enhancement of the (d, α) reaction (by a factor of ~ 3) over a pure $(s_{1/2}p_{1/2})^{-1}$ prediction and some lack of strength in the (t, α) transition imply considerable configuration mixing. This is in quantitative agreement

with Kuo's ground-state wave function

$$\psi(0)=0.906(3s_{1/2}{}^{\pi}3p_{1/2}{}^{\nu})^{-1}-0.315(2d_{3/2}{}^{\pi}3p_{3/2}{}^{\nu})^{-1}$$
$$+0.275(2d_{5/2}{}^{\pi}2f_{5/2}{}^{\nu})^{-1}-0.064(1g_{7/2}{}^{\pi}2f_{7/2}{}^{\nu})^{-1}.$$

Early shell-model calculations, for instance Kim's, predict a high purity, $0.99993(s_{1/2}p_{1/2})_{0-}$, for the ground state, and the dominant term $0.988(s_{1/2}p_{1/2})_{1-}$ for a first excited 1^- state at 66 keV. However, there is no reliable experimental evidence for a close ground-state doublet. In fact, the $(s_{1/2}{}^{-1}p_{1/2}{}^{-1})_{1-}$ configuration was found as the dominant component of the second excited state at 0.304 MeV.[8] Kuo's preliminary results[20] indicate a 0^-, 1^- splitting of 190 keV, which is in better agreement with experiment, but still too small.

1. $E_x=0.266$ *MeV.* This state is weakly excited by $l_n=3$ in (d,p), suggesting a J^π of 2^- or 3^-. In the (t,α) study, the level is poorly resolved from the 304-keV state although $l_p=2$ is postulated. Erskine's suggested assignment $J^\pi=2^-$ is supported by the lifetime measurement[5] for the $(E2)$ $2^-\rightarrow 0^-$ decay. Considerations of spectroscopic factors in (d,p) and (t,α) again are in agreement with 2^-. In $Pb^{208}(d,\alpha)$, this level is well resolved and very strongly excited by an enhanced, almost pure $L=3$ transition which definitely rules out 1^-. If the dominant amplitudes of this state are assumed to be $0.754(d_{3/2}p_{1/2})_{2-}$ and $0.554(s_{1/2}f_{5/2})_{2-}$ as calculated by Kuo, and found qualitatively by the stripping data, the $L=1$ component in (d,α) must, indeed, be much weaker than $L=3$. Kim's calculations too, predict strong configuration mixing for this 2^- state, however, he calculates the energy too high by 219 keV. In summary, the first excited state of Tl^{206} is strongly mixed $J^\pi=2^-$ state, very well described by Kuo's wave function and energy.

2. $E_x=0.304$ *MeV.* $Tl^{205}(d,p)Tl^{206}$ shows the strongest $l=1$ transition to this level which leads to a classification $(s_{1/2}p_{1/2})_{1-}$. The (d,α) reaction shows an enhanced pure $L=1$, $(0^-\leq J^\pi\leq 2^-)$ transition. Since the lowest 0^- and 2^- states have already been found, the (d,α) enhancement, (by a factor of about 2) also suggests $J^\pi=1^-$, in agreement with earlier assignments. Kuo calculates a slightly mixed state with $0.948(s_{1/2}p_{1/2})_{1-}$ as the dominant term. Kim's 1^- state lies 239 keV too low and would show no (d,α) enhancement.

3., 4. $E_x=0.636$, 0.652 *MeV.* This doublet has been well resolved only in the high-resolution γ-ray studies. In (d,p) it is marginally resolved, indicating measurable excitation of both levels. In (d,α) only the 0.636-MeV level is strongly excited, predominantly by $L=1$, hence $0^-\leq J^\pi\leq 2^-$. A $\sim$20% admixture of $L=3$ can either come from the 0.652-MeV level or indicate a 2^- assignment for the stronger state. The (t,α) data indicate $l_p=2$ for one of the levels, or $1^-\leq J^\pi\leq 3^-$. In the (n,γ) study a 635.3 keV level is found to decay to the 0.266 (2^-) and 0.304 (1^-) states, while a 0.650-MeV state decays to the 0.266 (2^-) level and ground state 0^-. With the usual assumption of dominating dipole decay, the level near 0.652 MeV must have $J=1$, while the level near 0.636-MeV could have $J=2$ or 1. The missing ground-state transition, however, indicates $J=2$. Both assignments are in agreement with the transfer data. The assignment of 2^- of the 0.636-MeV level is greatly strengthened by the observation that Kuo's wave function for the second 2^- state (calculated to be near 650 MeV) leads to a strongly enhanced $L=1$ (d,α) transfer. The 0.636-MeV $L=1$ transition is by far the strongest $L=1$ transfer observed, in excellent agreement with theory. (See Fig. 9.)

5. $E_x=0.806$ *MeV.* Excited through an $l=3$ transition in (d,p), a weak $l=2$ transition in (t,α), and a slightly enhanced pure $L=3$ transfer in d,α the state is limited to $2^-\leq J\leq 3^-$ by selection rules. The absence of an $L=1$ admixture in (d,α) and the lack of a primary γ ray to this state from the 0^+ or 1^+ resonance in $Tl^{205}(n,\gamma)$ are readily explained by the 3^- assignment. Kuo calculates a 3^- level at 0.81 MeV, in good agreement with the measured energy, however, details of the 3^- wave functions are not too well confirmed by experiment. The state appears to have a much more nearly pure configuration than indicated by Kuo's dominant amplitude $0.898(s_{1/2}f_{5/2})^{-1}$. There is little (d,α) enhancement and the cross section observed is about 2.3 times smaller than that predicted. The (t,α) reaction tests the $(d_{5/2}p_{1/2})^{-1}$ admixture of this state, and again it was found that this admixture is smaller than predicted.

6. $E_x=0.953$ *MeV.* This level has not been observed in other single-nucleon transfer reactions. In (d,α) it is populated by the only strong $L=5$ transition observed. In energy it corresponds reasonably closely to the 4^- level calculated at 1.04 MeV, which is the only predicted level nearby to fall within the experimental limit $4^-\leq J^\pi\leq 6^-$. Kuo's dominant two-hole amplitude $0.966(d_{3/2}f_{5/2})^{-1}$ explains the dominance (by about 70 to 1 for a pure configuration) of the $L=5$ contribution over $L=3$ as well as the fact that the level is not seen in direct reactions with Tl^{205} and Pb^{207} targets. Kim[8] predicts this 4^- state at about the same energy, but with a purity of 99.9%.

7. $E_x=0.999$ *MeV.* This level is excited by $l=3$ in (d,p) and by $l=2$ in (t,α) hence $2^-\leq J\leq 3^-$. The (d,α) angular distribution is a mixture of two L transfers. The $L=1$ component is distinct, and $J^\pi=2^-$ is unique, provided we do not have a a multiplet. The observed γ decay to the 0.266-MeV (2^-) level supports this assignment. The state corresponds well to a 2^- shell-model level near 1 MeV for which Kuo's as well as Kim's calculations predict much mixing predominantly $(s_{1/2}f_{5/2})^{-1}$ and $(d_{3/2}p_{1/2})^{-1}$. However, as we obtain uniform signs for the transition amplitudes only for the lowest J^π states, partial canceling results in a cross section without noticeable enhancement over transitions to states of a pure configuration, in agreement with experiment. A level at 1.080 MeV was reported in (n,γ) work, however, such a state has not been seen in any charged-particle study.

8. $E_x=1.12$ *MeV*. This level is measurably excited in (d, p) via $l=(3)$ and (t, α) by $l=2$, and decays through the 0.266-MeV (2^-) level, suggesting $J^\pi=2^-$, 3^-, or (1^-). The lower spins are favored because this level is populated by the primary decay of a 0^+ or 1^+ resonance in $Tl^{205}(n, \gamma)Tl^{206}$. The (d, α) cross section is so weak that this state is reported as uncertain. Apparently the relative phases in the amplitudes of configuration admixtures are such as to give rise to near cancellation of the transition amplitude. The shell-model state of Kuo at 1.43 MeV, $J^\pi=2^-$ yields the smallest cross section of the group of 2^- states examined. With rather minor changes in the amplitudes, this wave function could give vanishing cross section in (d, α). The drawback of a 2^- assignment is the unusually large difference (310 keV) between the calculated and measured level energy. If the tentative $l=(3)$ (d, p) assignment is disregarded, the state could be linked to the 1^- shell-model level predicted by Kuo at 1.20 MeV for which also almost complete cancellation in (d, α) is calculated.

9. $E_x=1.333$ *MeV*. This level is weakly excited in (d, p) and possibly in (t, α), but not seen in the (n, γ) experiment. The (d, α) transition is pure $L=1$, which limits J^π to $0^-\leq J\leq 2^-$. In energy and predicted transition strength, the state corresponds closely to Kuo's 1^- level calculated at 1.22 MeV. It is unlikely that it corresponds to the 1.20 level mentioned above. The 1.345-MeV level reported in (t, α) is poorly resolved in that experiment and may correspond to our 1.333-MeV state. If so the tentative $l_{t,\alpha}=2$ value would be consistent with our preferred 1^- assignment and eliminate the 0^- possibility.

10. $E_x=1.360$ *MeV*. The moderately strong (d, α) transition to this level is consistent with pure $L=1$. It is not resolved in (t, α) and seems weakly excited in (d, p). It γ-decays only through the 0.652- and 0.304-MeV 1^- states. All observations demand the limits $0^-\leq J^\pi\leq 2^-$ with a strong preference for 0^- and 1^-. A comparison with Kuo's calculated level scheme suggests strongly that this level is the second 0^- state (at 1.26 MeV) with the configuration

$$0.796(d_{3/2}p_{3/2})^{-1}-0.434(d_{5/2}f_{5/2})^{-1}+0.414(s_{1/2}p_{1/2})^{-1}+0.078(g_{7/2}f_{7/2})^{-1}.$$

The absence of an $L=3$ admixture and γ decays to $J>1$ states present good (but not conclusive) arguments for the 0^- assignment.

11. $E_x=1.406$ *MeV*. This level is not seen in (d, p) or (n, γ), but strongly excited by $l=5$ in (t, α), implying a significant $(h_{11/2}p_{1/2})^{-1}$ admixture. The (d, α) transition is very strong also. The main (d, α) stripping peak can be fitted by $L=(4)$, although the large-angle data are not reproduced by the DWBA curve (see Fig. 3). The large (d, α) cross section again is indicative of constructive interference of many transition amplitudes, and is well explained by Kuo's wave function for the lowest 5^+ state (1.44 MeV), as is the enhancement of the $L=4$ component over $L=6$. The uncharacteristically poor DWBA fit for $L=4$ is worrisome and indicates the need for further studies of large angular momentum transfers in (d, α); however, in view of the recent (t, α) results[10] this reassignment of J^π as compared to our tentative earlier interpretation[11] seems compelling.

12., 13., 14. $E_x=1.473$ *MeV* (*multiplet*). In (t, α) a small peak is partially resolved from level 11 and seems to show $l=2$ transfer. The (n, γ) reaction directly populates a level at 1.490 MeV, which decays to the 0.652-MeV (1^-) level, indicating a low spin state $J\leq 2$. The (d, α) reaction excites at least two levels at this energy with a summed angular distribution that strongly resembles $L=3$. The dominant contribution seems to come from a level near 1.473 MeV corresponding to the 3^- state [main term $0.706(d_{3/2}p_{3/2})^{-1}$] predicted for 1.44 MeV which supply about 60% of the observed (d, α) strength. A second closely spaced 3^- level (predicted for 1.46 MeV) could supply an additional 20% of the $L=3$ strength. The remaining observed strength may be attributable to the weak 2^- or a 1^- level also expected near this energy. The relatively poor $L=3$ fit and the (n, γ) data suggest the existence of an unresolved 1^- or 2^- state near 1.483 or 1.490 MeV; however, the experimental (d, α) resolution is insufficient to document more than two levels, and the assignment of level 14 is only based on the (n, γ) data.

15., 16. $E_x=1.623$ *MeV*. Figure 2 indicates at least two partially resolved states near 1.63 MeV. The partially resolved group at 1.649 MeV appears to correspond to a level seen in other studies and will be discussed further below. The main intensity of the 1.62-MeV multiplet, centers at 1.623 MeV and constitutes one of the strongest groups in the spectrum; it has, however, a rather unstructured, flat angular distribution, which can be reproduced by a number of combinations of two L values. With the assumption (made in Ref. 11) that the group corresponds to a single level, a mixture of $L=1$ and $L=3$ produced a reasonable fit. However, we have no way of explaining such a strong (2^-) level at this energy. Furthermore, the state is not observed in (d, p), (t, α), or (n, γ) studies, which leads us to conclude that the main intensity must come from a high spin level which is not excited in these reactions. Kuo's preliminary shell-model calculations yield such a high spin level at 1.63 MeV—the lowest 7^+ state—with a wave function

$$0.796(s_{1/2}i_{13/2})^{-1}+0.389(h_{11/2}p_{3/2})^{-1}+0.324(d_{3/2}i_{13/2})^{-1}-0.230(h_{11/2}f_{5/2})^{-1}+0.175(d_{5/2}i_{13/2})^{-1}+0.151(h_{11/2}f_{7/2})^{-1}+0.049(g_{7/2}i_{13/2})^{-1}-0.028(h_{11/2}h_{9/2})^{-1}.$$

It is clear that neither $Tl^{205}(d, p)$ nor $Pb^{207}(t, \alpha)$ are likely to excite this level directly. On the other hand, a 6^+ state, such as the one predicted at 1.75 MeV is likely to be excited by (t, α), while the lowest 8^+ state

is not expected until 2.11-MeV excitation. Hence, there is strong indirect evidence that the observed group at 1.623 MeV contains the 7^+ state. Kuo's wave function listed above predicts strong coherent enhancement for this 7^+ state [by a factor of 4 over a pure $(s_{1/2}i_{13/2})^{-1}$ configuration], in good agreement with experiment, while no other nearby state would be similarly enhanced. However, Kuo's 7^+ state also would be almost exclusively excited by $L=6$. The 1.623-MeV angular distribution certainly is not pure $L=6$ and we suggest that its structure is washed out by an unresolved $L=3$ transition which could for instance populate the 2^- level expected near 1.62 MeV. A tentative decomposition is shown in Fig. 3. Such an interpretation would be in agreement with Kuo's calculation and with existing data, in particular with the low spin level observed at 1.631 MeV in (n,γ); however, it is certainly desirable to establish more directly that the 1.623-MeV group does, indeed, contain the postulated doublet.

17. $E_x=1.649$ *MeV.* This relatively weak level is not always well resolved from the strong neighboring 7^+ state, but the data show a definite deep minimum at $\theta=20°$. Only $L=6$ or $L=1$ calculations show a minimum at this angle. The same state seems to be observed in (t,α) with $l=2$ at 1.657 MeV. This would only permit the $L=1$ fit, which limits the state of $J^\pi=0^-, 1^-, 2^-$. The level could correspond to the 1^- shell-model state expected at 1.47 MeV which has not been accounted for. Theoretically, its strongest components are $0.929(d_{3/2}p_{3/2})^{-1}+0.306(d_{3/2}p_{1/2})^{-1}$ so that this state can be seen in (t,α) with $l=2$. The marked (180-keV) energy discrepancy between experiment and calculation is only a little larger than that for other 1^- states. The energies of all 1^- levels, surprisingly, seem to be predicted much more poorly than those for other J^π values.

18. $E_x=1.712$ *MeV.* Excited a strong $l=5$ in (t,α) the state is believed to be primarily composed of the $(h_{11/2}p_{1/2})^{-1}$, $J^\pi=6^+$ configuration. The (d,α) distribution peaks at $\approx 35°$ in agreement with the DWBA $L=6$ prediction, although, as in the 1.406-MeV $L=4$ case the experimental slope of the distribution is steeper than predicted. The magnitude of the $L=6$ distribution is enhanced by about 1.5, compared to a pure configuration. This indicates moderate configuration mixing in agreement with the Kuo's shell-model wave function for the 1.75-MeV 6^+ state which predicts an enhancement factor of 2.

19. $E_x=1.800$ *MeV.* Not excited in (t,α) or (d,p), this level yields an (d,α) angular distribution consistent with $L=2+4$ mixtures. Although the deep minimum at 57° is not reproduced by the the DWBA, it is similar to the empirical distribution for the $L=4$, 1.406-MeV level. Thus, $J^\pi=3^+$ is implied, consistent with the absence of the level in (t,α), since only $J=5$ and 6 can be reached for positive-parity states by proton pickup from the $Z=50$–82 shell. This level appears to correspond to the 1.88-MeV 3^+ shell-model level of Kuo. The lack of $L=4$ strength implied by the $(h_{11/2}f_{5/2})^{-1}$ shell-model wave function appears to be in disagreement with experiment, and this gives rise to the discrepancy in intensities at 40° shown in Fig. 9.

20. $E_x=1.845$ *MeV.* Strongly excited in (t,α) through $L=2$, this level is expected to have a large $(d_{5/2}p_{1/2})^{-1}$ component. The dominant $L=1$ strength in (d,α) excludes $J^\pi=3^-$. This spin ordering of the $(d_{5/2}p_{1/2})^{-1}$ doublet is reproduced by the shell-model calculations although the predicted 1.99-MeV 2^- level lies at a somewhat higher excitation than observed. The $L=1$ dominance over $L=3$ is predicted by the wave function.

21. $E_x=1.983$ *MeV.* This level is weakly excited through $l=5$ in (t,α). The (d,α) angular distribution had previously[11] been compared to $L=3$, but additional measurements at larger angles show a steep falloff in better agreement with $L=4$, which would be consistent with (t,α) and would indicate $J^\pi=(5^+)$. The 5^+ shell-model state at 2.12 MeV consists of a rich mixture of $(d_{3/2}i_{13/2})^{-1}$ and $(h_{11/2}p_{1/2})^{-1}$ configurations, both of which favor $L=4$ by more than an order of magnitude over $L=6$ in (d,α). The transition strength is in fair agreement with the experimental value (Fig. 9).

22. $E_x=2.058$ *MeV.* Excited strongly via $l=2$ in (t,α) this state is populated by $L=(3)$ in (d,α) and is likely to be the 3^- member of the $(d_{5/2}p_{1/2})^{-1}$ doublet. While the experimental transition is of average strength, Kuo's wave function for the corresponding 3^- level at 2.09 MeV predicts strong cancellation. The absence of such cancellation as well as the small observed enhancement of the lowest 3^- level may indicate too much configuration mixing in the theoretical 3^- states.

23. $E_x=2.080$ *MeV.* This previously unreported level has an almost flat angular distribution, which agrees well with the calculated $L=8$ DWBA curve. To be visible the $L=8$ transition would have to be enhanced. Hence the level probably corresponds to the 2.11-MeV 8^+ shell-model state with $(h_{11/2}f_{5/2})^{-1}$ as a dominant configuration. The theoretical and empirical level energies agree surprisingly well.

26. $E_x=2.217$ *MeV.* Previously unreported, this is the most strongly excited of all neutron-proton hole levels. It is very encouraging that such a strong level is accurately predicted by the constructively coherent amplitudes of the 2.05-MeV 4^- shell-model wave function. One also predicts an almost pure $L=3$ transition, in perfect agreement with experiment. (See Figs. 3 and 9.)

Remaining $\pi^{-1}\nu^{-1}$ Levels

Of the many remaining levels, most are weakly excited and their L transfer and correspondence to the shell-model states are less certain. This does not preclude the possibility that some of these higher-lying states are collective states of high spin such as 6^-, 7^-, 8^-, and 9^+. However, the level density is too high to expect sufficient level isolation for good angular distributions. This is especially true for high-spin angular distributions

which tend to have little structure, as previously noted for $L=5$ and $L=8$, and as expected for $L=7$ and 9.

Three-Hole–One-Particle States

As noted in the (d, p) studies of Erskine,[8] the strong states at 2.581 and 2.594 MeV are expected to be primarily the $s_{1/2}^{-1}g_{9/2}$ configuration coupled to the Pb^{206} core. It is clear (Fig. 2) that this doublet is not excited in the $Pb^{208}(d, \alpha)Tl^{206}$ reaction. It is interesting to note that the particle-hole interaction appears much weaker than the two-hole interaction as evidenced by the 13-keV spread of this particle-hole doublet compared to the separations of several hundred keV seen for the hole-hole doublets.

VI. SUMMARY AND CONCLUSIONS

Nearly all of the expected low-lying $\pi^{-1}\nu^{-1}$ states of Tl^{206} have been observed via the $Pb^{208}(d, \alpha)Tl^{206}$ reaction at 17 MeV. With 14-keV α resolution we have been able to separate and analyze most of the levels below $\sim$2.5-MeV excitation, which should greatly aid the understanding of this two-hole nucleus. With the help of recent shell-model wave functions[20] and microscopic DWBA calculations, it was possible to identify details of the Tl^{206} wave functions and to suggest a value for the absolute (d, α) cross-section normalization N.

We find that the nuclear interior cannot be neglected in (d, α) DWBA work, and that finite-range and nonlocality corrections help to bring theory into better agreement with measured cross sections. However, most constituent π-ν configurations seem to have a minor effect on the relative angular distributions. Also, firm evidence for spin-orbit effects has not been found in the data. While most angular distributions are predicted surprisingly well, some difficulties with $L=4$ and 6 were noted and are not well understood.

Considerable variations in the absolute cross sections are seen to be a direct result of the configuration admixtures. The shell-model spectrum of Tl^{206} is characterized by a low-lying "π-ν vibration" or deuteron-enhanced state for each $J^\pi(L)$ value in good agreement with experiment. The only serious discrepancy between shell-model expectations and this work is that the predicted collective $L=5$ transition for $J^\pi=5^-$ was not found below 2.5 MeV. The principal (d, α) strength for this state comes from two configurations involving the $2d_{5/2}$ and $2f_{7/2}$ orbitals. There is evidence from (d, t), (d, He^3), and (t, α) reactions on Pb^{208} that the highly excited hole states such as $2d_{5/2}$ and $2f_{7/2}$ are not pure, and this may be a partial explanation of the problem.

Other less serious discrepancies between data and theory may imply that configuration admixtures in Kuo's wave functions[20] have been somewhat overestimated. This is especially true of the 3^- state at 0.806 MeV where the lack of collective strength in (d, α) as well as the small (t, α) spectroscopic factor[10] indicate an overestimate of the $d_{5/2}^{-1}p_{1/2}^{-1}$ admixture.

We conclude that the $Pb^{208}(d, \alpha)Tl^{206}$ reaction has been amenable to a microscopic DWBA analysis, and that characteristic properties of the reaction observed for Pb^{208} may well be anticipated for other heavy- and medium-weight nuclei. However, it is clear that our estimate of $N(d, \alpha)\approx 20$ depends very much on calculational parameters such as β_d, β_α, $R_{d,\alpha}$, the α-particle size assumed, the bound-state proton potential well, and the continuous ambiguity in the α- and possibly deuteron optical-model parameters; and further studies of these parameters and their effect on N are called for.

Our observation of coherent enhancement of the lowest states for each value of J^π is direct evidence for appreciable configuration mixing of the low-lying states of Tl^{206}, and its interpretation is quite independent of the DWBA calculations used. While Kim's early, very pure two-hole wave functions[8] for Tl^{206} cannot possibly explain some of the observed variations in transition strengths for a given J and L, Kuo's more recent, strongly mixed functions do rather well, with the few exceptions noted above. It will be of great interest to see if future calculations with realistic forces and higher-order corrections will give even more realistic configuration admixtures while removing some of the discrepancies in the calculated and measured level energies, which seem particularly large for the 1^- states.

ACKNOWLEDGMENTS

It is a pleasure to acknowledge helpful discussions with Dr. R. M. Drisko and Dr. F. Rybicki throughout the analysis of the data. We also wish to thank Dr. Y. S. Park for assistance in the data acquisition.